Binding Kinetics and Ligand Specificity for the Interactions of the C2B Domain of Synaptogmin II with Inositol Polyphosphates and Phosphoinositides†

Bharat Mehrotra,‡ David G. Myszka,§ and Glenn D. Prestwich*,‡

Department of Medicinal Chemistry, The University of Utah, 30 South 2000 East, Room 201, Salt Lake City, Utah 84112-5820, and Department of Oncological Sciences, The University of Utah Huntsman Cancer Institute, 50 North Medical Drive, School of Medicine, 4A417, Salt Lake City, Utah 84132

Received March 2, 2000; Revised Manuscript Received May 9, 2000

ABSTRACT: Synaptotagmin II (Syt II) is a key protein in the calcium-dependent exocytosis of synaptic vesicles. It contains two domains homologous to the C2 regulatory region of protein kinase C. The C2A domain acts as a calcium sensor, while the C2B domain has high affinity for inositol polyphosphates ($InsP_n$s) and phosphoinositide polyphosphates ($PtdInsP_n$s). We describe the use of a surface plasmon resonance biosensor in determining the binding kinetics of the C2B domain with $InsP_n$ and $PtdInsP_n$ ligands. Biosensor surfaces were prepared with covalently attached Ins(1,4,5)P_3, Ins(1,3,4,5)P_4, and $InsP_6$ ligands. The interactions of bacterially expressed His_6-tagged C2B and (C2A+C2B) domains of Syt II were examined in the presence and absence of competing $InsP_n$s and $PtdInsP_n$s. Both His_6-C2B and His_6-(C2A+C2B) exhibited the highest affinity for the Ins(1,3,4,5)P_4-modified surface with a K_D value of 6 nM. The His_6-(C2A+C2B) had a 10-fold lower association rate constant for the $InsP_6$-linked surface ($k_a = 4.6 \times 10^3$ M^{-1} s^{-1}) than for the Ins(1,3,4,5)P_4-modified surface ($k_a = 6.8 \times 10^4$ M^{-1} s^{-1}). Two water-soluble phosphoinositides, dioctanoyl-PtdIns(3,4,5)P_3 and dioctanoyl-PtdIns(4,5)P_2, were superior to the soluble $InsP_n$s in displacing binding to the Ins(1,3,4,5)P_4-modified surface. The binding of His_6-C2B and His_6-(C2A+C2B) to $InsP_n$ surfaces did not show significant calcium dependence. These data support a model in which the binding of the C2B domain of Syt II to $PtdInsP_n$s is important for the docking and/or fusion of the secretory vesicles to the synaptic plasma membrane.

Synaptotagmins are integral membrane proteins of secretory vesicles, abundant in neural and some endocrine cells, and comprise more than 12 isoforms with diverse functions in tissue-specific expressions (*1*, *2*). Synaptotagmins appear to regulate vesicle exocytosis, although they may also be important in endocytosis (*3*). The cytoplasmic domain of each isoform contains two copies of highly conserved repeats that are homologous to the C2 regulatory region of protein kinase C (*4*). The two C2 domains are involved in both calcium-dependent and calcium-independent interactions (Figure 1). The C2A domain of several synaptotagmins binds phospholipids in the presence of calcium (*5*). This interaction implicates synaptotagmin as a calcium sensor in the exocytosis pathway of the synaptic vesicle cycle (*6*, *7*). The C2A domain also binds a plasma membrane protein, syntaxin, in the presence of calcium (*8*, *9*). This binding is necessary for the exocytosis of synaptic vesicles.

The C2B domain appears to play several roles. First, the C2B domain was reported to bind inositol polyphosphates

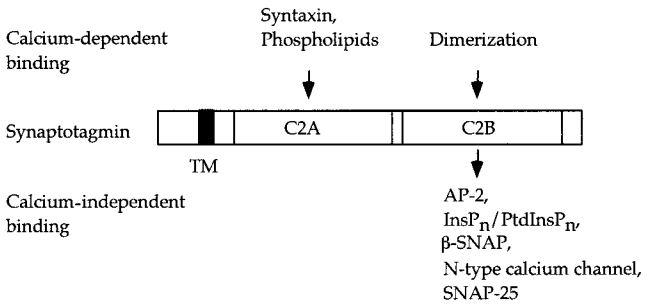

FIGURE 1: Calcium-dependent and calcium-independent binding of synaptotagmin with proteins and lipids.

($InsP_n$s)[1] and phosphoinositide polyphosphate ($PtdInsP_n$) ligands (*10*, *11*). This binding of the $InsP_n$s was not calcium-dependent, but a calcium concentration-dependent switch of binding affinity from PtdIns(3,4,5)P_3 at low calcium concentrations to PtdIns(4,5)P_2 (>10 μM calcium) was reported

† This work was supported by Grant NS-29632 from the National Institutes of Health (to G.D.P.). D.G.M. thanks The Huntsman Cancer Institute and The University of Utah Cancer Center Support Grant (National Cancer Institute, Grant 5P30 CA42014) for support of the BIACORE instrumentation facility.

* To whom correspondence should be addressed: Department of Medicinal Chemistry, The University of Utah, 30 South 2000 East , Room 201, Salt Lake City, UT 84112-5820. Phone: (801) 585-9051. Fax: (801) 585-9053. E-mail: gprestwich@deans.pharm.utah.edu.

‡ The University of Utah.

§ The University of Utah Huntsman Cancer Institute.

[1] Abbreviations: AP-2, assembly protein-2; BIA, biomolecular interaction analysis; GST, glutathione *S*-transferase; His_6, histidine-tagged; Ins(1,3,4,5)P_4, inositol 1,3,4,5-tetrakisphosphate; Ins(1,4,5)P_3, inositol 1,4,5-trisphosphate; $InsP_6$, inositol hexakisphosphate; $InsP_n$, inositol polyphosphate; NHS, *N*-hydroxysuccinimide; EDC, *N*-ethyl-*N*′-[3-(*N*,*N*-dimethylamino)propyl]carbodiimide; PAGE, polyacrylamide gel electrophoresis; PtdIns(3,4)P_2, phosphatidylinositol 3,4-bisphosphate; PtdIns(3,4,5)P_3, phosphatidylinositol 3,4,5-trisphosphate; PtdIns(4,5)P_2, phosphatidylinositol 4,5-bisphosphate; $PtdInsP_n$s, phosphatidylinositol polyphosphates, or phosphoinositides; SDS, sodium dodecyl sulfate; SNAP, soluble NSF attachment protein; Syt II, synaptotagmin II.

10.1021/bi000487o CCC: $19.00
Published on Web 07/20/2000

for a liposome model system (*12*). Second, the C2B domain was shown to bind clathrin assembly protein-2 (AP-2), and this was reported to play an essential role in endocytosis of synaptic vesicles (*13*), an interaction regulated by $InsP_n$s (*14*). The evidence from the defective recycling of synaptic vesicles in synaptotagmin mutants of *Caenorhabditis elegans* directly supported a role for synaptotagmin in endocytosis (*15*). Third, the C2B domain of synaptotagmin bound to two plasma membrane proteins, soluble NSF attachment protein (β-SNAP) (*16*) and SNAP-25 (*17*, *18*). Fourth, the C2B domain of synaptotagmin was reported to bind to N-type calcium channels (*19*, *20*). This interaction might be important in the docking of synaptic vesicles close to the active zone. Fifth, synaptotagmin was found to self-associate in a calcium-dependent process by forming both homo- and heterodimers (*21*, *22*). Self-association was mediated by the C2B domain, but required the integrity of the entire synaptotagmin molecule for maximal effect (*23*). Thus, synaptotagmin not only acts as a calcium sensor but also has a central role in both lipid−protein and protein−protein interactions in the process leading to exo- and endocytosis of synaptic vesicles.

We previously reported (*11*) the photoaffinity labeling of the C2B domain of murine Syt II with a series of benzophenone-containing aminoalkyl-modified $InsP_n$ derivatives (*24*, *25*). These studies established the headgroup selectivity of the C2B domain and localized a base-rich 32-mer polypeptide as the important binding region within the C2B domain. However, no kinetic data were obtained from this study, since photoaffinity labeling is intrinsically a nonequilibrium process. One current hypothesis is that $InsP_6$ or other "high $InsP_n$s" (*26*) are the key ligands for the C2B domain, and that the interaction of $InsP_6$ or other polyphosphates with the C2B domain acts as an endocytotic block prior to the entry of calcium and release of the block. To further examine this hypothesis, a real-time binding method was required to establish both the kinetics of the C2B−$InsP_n$ interactions and the selectivity of the C2B domain for $InsP_n$ versus $PtdInsP_n$ ligands. We describe herein the preparation and use of $InsP_n$ covalently modified surface plasmon resonance biosensor to determine the kinetics of the binding of $InsP_n$s with either the C2B or the (C2A+C2B) domain of Syt II. This biosensor was used to examine the Ca^{2+} dependency of the binding of the C2B domain to $InsP_n$ surfaces, and to probe the kinetic ligand specificity of the C2B domain.

EXPERIMENTAL PROCEDURES

Chemicals. 1-*O*-(3-Aminopropyl)-D-*myo*-Ins(1,4,5)P_3, 1-*O*-(3-aminopropyl)-D-*myo*-Ins(1,3,4,5)P_4, 1-*O*-(6-aminohexyl)-D-*myo*-$InsP_6$, D-*myo*-Ins(1,4,5)P_3, and D-*myo*-Ins(1,3,4,5)P_4 were prepared as described previously (*27*−*30*). Dioctanoyl (di-C_8) PtdIns(4,5)P_2 and di-C_8 PtdIns(3,4,5)P_3 (*24*, *31*) were provided by Echelon Research Laboratories, Inc. (Salt Lake City, UT), and $InsP_6$ was obtained from Sigma Chemical Co. (St. Louis, MO). BIACORE 2000, PIONEER sensor chip B1, *N*-hydroxysuccinimide (NHS), and 3-(*N*,*N*-dimethylamino)propyl-*N*-ethylcarbodiimide (EDC) were purchased from BIACORE Inc. (Uppsala, Sweden). All other chemicals were reagent grade commercial products. Solutions were prepared using Nanopure (ultrafiltered, distilled, and deionized) water.

Preparation of Ins(1,4,5)P_3, Ins(1,3,4,5)P_4, and $InsP_6$ Chips. The aminoalkyl $InsP_n$ derivatives were covalently coupled to a carboxymethyldextran-coated BIACORE sensor chip (PIONEER sensor chip B1) using standard carbodiimide chemistry (*32*). The surface was first activated with a 7 min injection of a mixture of 0.1 M NHS and 0.1 M EDC in water. The Ins(1,4,5)P_3 surface was then created by reaction of the activated surface with an aqueous solution of 1-*O*-(3-aminopropyl)-D-*myo*-Ins(1,4,5)P_3 for 30 min at 2 μL/min. After the coupling step, the remaining activated groups were blocked with a 7 min wash of 1 M ethanolamine. Control flow cells were activated and deactivated using the same chemistry, but without the aminoalkyl $InsP_n$. The Ins(1,3,4,5)P_4 and $InsP_6$ chips were prepared in an analogous fashion using the appropriate aminoalkyl $InsP_n$ derivative.

Nonspecific Binding and Mass Transport Effect. GST-C2B was passed over the unmodified sensor chips CM5 and PIONEER sensor chip B1 at 100 μL/min for 50 s. The surface was regenerated by washing with 50 μL of 6 M guanidinium-HCl, 50 μL of 0.05% sodium dodecyl sulfate (SDS), and 50 μL of 5 M NaCl. To determine a mass transport effect, His_6-C2B was passed over the Ins(1,3,4,5)P_4 surface at rates of 33 and 100 μL/min.

Construction, Expression, and Purification of Fusion Proteins. Glutathione *S*-transferase (GST) constructs of Syt II C2B and Syt II (C2A+C2B) were obtained from K. Mikoshiba and M. Fukuda (The University of Tokyo, Tokyo, Japan), and the proteins were expressed and purified as described previously (*11*). Using the GST-C2B plasmid as a template, the His_6-tagged construct of Syt II C2B was obtained by PCR (sense, 5′-CGCGGCAGCCATATGGGAGGAGGAGAGAAGGAGCCAGAG-3′; and antisense, 5′-CTCGAGGAATTCTTACTAGTCGGACCAGTGCCGCAA-3′, designed such that it contains an *Nde*I cleavage site at the 5′-end and an *Eco*RI cleavage site at the 3′-end) for 35 cycles, each involving denaturation at 94 °C for 2 min, annealing at 55 °C, and extension at 72 °C for 3 min. Similarly, using the GST-(C2A+C2B) plasmid as a template, the His_6-tagged construct of Syt II (C2A+C2B) was obtained by PCR (sense, 5′-CGCGGCAGCCATATGGGAGGAGGAGAGCCAGCGAACCTGGGC-3′; and antisense, 5′-CTCGAGGAATTCTTAATCGTCGGACCAGTGCCGCAA-3′, designed such that it contains an *Nde*I cleavage site at the 5′-end and an *Eco*RI cleavage site at the 3′-end) for 35 cycles, each involving denaturation at 94 °C for 2 min, annealing at 55 °C, and extension at 72 °C for 3 min. The amplified fragments were subcloned into a pET 28a(+) vector and verified by DNA sequencing.

NovaBlue (DE3) *Escherichia coli* cells were electroporated and transformed with purified plasmids. Cells were grown in Luria broth with kanamycin and induced with isopropyl 1-thio-β-D-galactopyranoside, and the expressed proteins were purified by Ni^{2+} chelate chromatography (Novagen, Inc., Madison, WI) according to the manufacturer's recommendations. The proteins were further purified by gel filtration (Superdex 75) chromatography in Tris buffer [50 mM Tris-HCl and 100 mM NaCl (pH 7.4)] and analyzed by 10% SDS−polyacrylamide gel electrophoresis (PAGE).

Kinetic Studies of C2B and (C2A+C2B) Binding to $InsP_n$ Chips. All biosensor experiments were performed in a buffer containing 50 mM Tris, 100 mM NaCl, and 0.005% Tween 20 at pH 7.4 and 25 °C. The kinetic studies were performed in triplicate using five successive 3-fold dilutions of the same protein. The flow rate was maintained at 33 μL/min. The

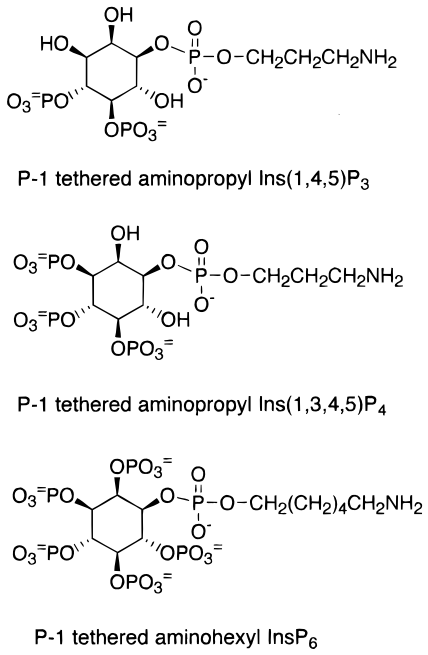

FIGURE 2: Structure of different amino-tethered InsP$_n$s used for BIACORE studies.

dissociation data were collected for 300 s. The surfaces were regenerated by washing with 25 μL of 6 M guanidinium-HCl, 25 μL of 0.05% SDS, and 25 μL of 5 M NaCl after each run.

Competitive Displacement Studies. Different competitors were preincubated with the His$_6$-tagged fusion protein at 4 °C for 15 min and were then passed over the Ins(1,3,4,5)P$_4$ surface. Surfaces were then regenerated as described above.

Ca^{2+}-Dependent Studies. The protein samples were incubated with 1 mM Mg^{2+} and 0, 10, 20, 50, 100, 250, and 500 μM Ca^{2+}. The samples were then passed over the Ins(1,3,4,5)P$_4$ surface at a rate of 33 μL/min in a Tris buffer that contained 1 mM Mg^{2+}. All experiments were performed in triplicate.

RESULTS

Preparation of Ins(1,4,5)P$_3$, Ins(1,3,4,5)P$_4$, and InsP$_6$ Sensor Chips. Three different aminoalkyl-tethered InsP$_n$ ligands (*33*, *34*) were used to covalently modify carboxymethyldextran-coated BIACORE sensor chips. These include P-1-tethered 3-aminopropyl Ins(1,4,5)P$_3$ (*28*, *35*), the P-1-tethered 3-aminopropyl Ins(1,3,4,5)P$_4$ (*29*, *36*), and P-1-tethered 6-aminohexyl InsP$_6$ (*27*) as shown in Figure 2. A preliminary report using a similar approach to prepare sensor chips to assess binding of the Ins(1,4,5)P$_3$ receptor cytoplasmic binding domain was published independently during the preparation of this paper (*37*). The tethered InsP$_n$ affinity resins have been extensively employed in purification of native and recombinant InsP$_n$ and PtdInsP$_n$ binding proteins and enzymes (*33*, *34*, *38*−*41*). Each sensor chip has four different flow cells. Two flow cells were used to attach the InsP$_n$s, while the other two flow cells were kept as controls. Binding to the control flow cells was subtracted from the experimental flow cells to determine the amount of nonspecific protein binding. This aminoalkyl linker provided sufficient flexibility and accessibility of the InsP$_n$ headgroup to allow binding of proteins in the mobile phase. Moreover, it is important to note that this system partially mimics a phosphoinositide in that a P-1 three-carbon linker is present rather than the free P-1 phosphodiester (*33*). The optimal loading for the tethered InsP$_n$ on each sensor chip type was empirically determined.

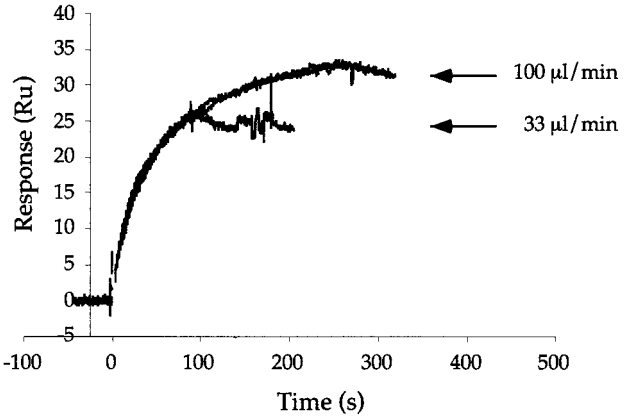

FIGURE 3: Mass transport effect. His$_6$-C2B was passed over the InsP$_6$ surface at rates of 33 and 100 μL/min. No flow rate dependence was observed since the association curves perfectly overlay on each other. The jump in the dissociation curve at 33 μL/min is due to an air bubble.

Nonspecific Binding. Two carboxymethyldextran-coated surfaces, CM5 and PIONEER sensor chip B1, were employed. To determine the amount of nonspecific binding of these proteins, GST-C2B was passed over these unmodified surfaces. The PIONEER sensor chip B1 exhibited a much lower level of nonspecific binding when compared with the CM5 chip (data not shown). This low background binding can be attributed to the lower loading of free carboxylic groups on the surface, with a 10-fold lower density on the PIONEER sensor chip B1 than on the CM5 chip. All subsequent quantitative biomolecular interaction analyses were thus performed with the PIONEER sensor chip B1.

Mass Transport Effect. One advantage of using surface plasmon resonance is that the reactants do not need to be labeled with radioactive or spectroscopic probes. However, a disadvantage is that one of the binding partners must be covalently attached to a sensor chip surface. This limits the ability to accurately determine rate constants for rapid processes, since the reactant in solution must first be transported by diffusion to the surface to bind to its immobilized partner. If diffusion (*42*) is much faster than the association of analyte with the bound ligand, then mass transport is not limiting and thus does not affect the interaction being monitored. To determine if mass transport was limiting, the His$_6$-C2B fusion protein was passed over the Ins(1,3,4,5)P$_4$ surface at two flow rates, 33 and 100 μL/min. No change in the association curve for these two flow rates was observed, thus suggesting the absence of a mass transport effect (Figure 3).

Kinetic Studies of C2B and (C2A+C2B) Binding to InsP$_n$ Chips. To determine the kinetics of the interaction between the protein and InsP$_n$ surface, the proteins were passed over the surface at five different concentrations. The data were analyzed using nonlinear least-squares global fitting software (*43*). The observed data were fitted to a single-site interaction model. The obtained kinetic values are shown in Table 1. An extremely close fit was observed for the binding of His$_6$-C2B and His$_6$-(C2A+C2B) to Ins(1,3,4,5)P$_4$ and InsP$_6$

Table 1: Kinetic Studies into the Binding of (A) His_6-C2B and (B) His_6-(C2A+C2B) to Different $InsP_n$ Surfaces[a]

	k_a (M^{-1} s^{-1})	k_d (s^{-1})	K_D (nM)
(A) His-C2B Binding to an $InsP_n$ Surface			
$Ins(1,4,5)_3$	3.7×10^4	8.0×10^{-4}	14
$Ins(1,3,4,5)P_4$	8.1×10^4	4.9×10^{-4}	6
$InsP_6$	4.6×10^4	3.9×10^{-4}	8.5
(B) His-(C2A+C2B) Binding to an $InsP_n$ Surface			
$Ins(1,4,5)_3$	3.3×10^4	6.2×10^{-4}	18.7
$Ins(1,3,4,5)P_4$	6.8×10^4	3.5×10^{-4}	5.1
$InsP_6$	4.6×10^3	3.5×10^{-4}	76

[a] The kinetic parameters were obtained using nonlinear least-squares global fitting. The observed data were fitted to a single-site interaction model. This gave the association rate constant (k_a) and the dissociation rate constant (k_d), which then gave the equilibrium dissociation constant (K_D).

surfaces, while the binding to $Ins(1,4,5)P_3$ surface was less ideal (Figures 4 and 5). The rate constants allowed the calculation of a K_D value in the low nanomolar range for the binding of His_6-C2B to $Ins(1,3,4,5)P_4$ and $InsP_6$ chips, while the binding to $Ins(1,4,5)P_3$ occurred with a slightly lower affinity. Interestingly, for His_6-(C2A+C2B), it was observed that the association rate for the $InsP_6$ surface was 10-fold lower than that for the $Ins(1,4,5)P_3$ and $Ins(1,3,4,5)P_4$ surfaces, leading to a correspondingly higher K_D value. Since the $Ins(1,4,5)P_3$ and $Ins(1,3,4,5)P_4$ surfaces mimic $PtdIns(4,5)P_2$ and $PtdIns(3,4,5)P_3$, respectively, this result supports the notion that $PtdIns(4,5)P_2$ and $PtdIns(3,4,5)P_3$ might have a higher affinity than $InsP_6$ in vivo.

Similar experiments were performed with GST fusion proteins of C2B and (C2A+C2B). However, complications in interpretation of the data arise because the GST fusion partner can dimerize. These avidity effects mitigate against proper calculation of kinetic values. To circumvent this difficulty, only His_6-tagged fusion proteins were used in the kinetic studies described here.

Competition Studies. To determine the selectivity of the C2B domain for different inositide ligands, competition studies were performed using $Ins(1,4,5)P_3$, $Ins(1,3,4,5)P_4$, $InsP_6$, di-C_8 $PtdIns(4,5)P_2$, and di-C_8 $PtdIns(3,4,5)P_3$. Di-C_8 $PtdIns(4,5)P_2$ and di-C_8 $PtdIns(3,4,5)P_3$ are water-soluble analogues of the natural lipids. These analogues exhibit no tendency to form micelles. His_6-(C2A+C2B) was preincubated with each competitor at 10 μM at 4 °C for 15 min to generate a competitor−C2B complex. This sample was then passed over the $Ins(1,3,4,5)P_4$ surface. The di-C_8 $PtdIns(4,5)P_2$ and di-C_8 $PtdIns(3,4,5)P_3$ ligands almost completely abrogated binding of C2B to the biosensor chip. In contrast, the soluble headgroups $Ins(1,4,5)P_3$ and $Ins(1,3,4,5)P_4$ were much less efficient competitors (Figure 6). $InsP_6$ was found to be a stronger competitor than $Ins(1,4,5)P_3$ and $Ins(1,3,4,5)P_4$.

Ca^{2+} Dependency of Binding. Synaptotagmin has both C2A and C2B domains, but only the C2A domain exhibits calcium-sensitive sensor phospholipid binding (*5*, *7*, *44*). The C2B domain of Syt I behaved as a calcium sensor in vitro, binding to $PtdIns(3,4,5)P_3$-containing liposomes at submicromolar Ca^{2+} concentrations and to $PtdIns(4,5)P_2$-containing lipids at Ca^{2+} concentrations of >10 μM (*12*). Thus, the calcium-dependent binding of Syt II C2B to $InsP_n$ surfaces was explored, using 1 mM $MgCl_2$ to buffer the effects of changing divalent cation concentrations. These conditions approximate the physiological levels of Mg^{2+} present at the nerve terminals. The proteins were incubated with different concentrations of Ca^{2+} for 15 min at 4 °C and then passed over the $Ins(1,3,4,5)P_4$ surface. We found that increased Ca^{2+} concentrations only modestly increased the affinity of His_6-C2B for the $Ins(1,3,4,5)P_4$ surface (Figure 7). Similar increases in the extent of binding of His_6-C2B to other $InsP_n$ surfaces was also observed, although there was no significant shift in the binding affinities (data not shown). Similarly, to study whether the calcium concentration affects the binding of $InsP_n$s to the C2B domain in the presence of the C2A domain, His_6-(C2A+C2B) was examined. Only a slight increase in the extent of binding of His_6-(C2A+C2B) to the $Ins(1,3,4,5)P_4$ surface was observed above 10 μM Ca^{2+} (Figure 8). This modest increase suggested that Ca^{2+} might not significantly affect the binding of $InsP_n$ to the C2B domain of Syt II.

DISCUSSION

To obtain kinetic data on the binding of $InsP_n$s and $PtdInsP_n$s to the C2B domain, surface plasmon resonance biosensor surfaces were prepared with covalently attached $Ins(1,4,5)P_3$, $Ins(1,3,4,5)P_4$, and $InsP_6$ ligands. Biomolecular interaction analysis of bacterially expressed His_6-tagged C2B and (C2A+C2B) domains of Syt II was then carried out in the presence and absence of competing $InsP_n$s and $PtdInsP_n$s. Both His_6-C2B and His_6-(C2A+C2B) showed the highest affinity for a *P*-1-(*O*-3-aminopropyl) $Ins(1,3,4,5)P_4$-modified surface with a K_D value of 6 nM. The His_6-(C2A+C2B) had a 10-fold lower association rate constant for the $InsP_6$-linked surface ($k_a = 4.6 \times 10^3$ M^{-1} s^{-1}) than for the $Ins(1,3,4,5)P_4$-modified surface ($k_a = 6.8 \times 10^4$ M^{-1} s^{-1}). Two water-soluble phosphoinositides, di-C_8 $PtdIns(3,4,5)P_3$ and di-C_8 $PtdIns(4,5)P_2$, competitively displaced binding of His_6-C2B to the $Ins(1,3,4,5)P_4$-modified surface and showed more potent displacement than the "headgroup only" $InsP_n$s. Finally, the binding of His_6-C2B and His_6-(C2A+C2B) to different $InsP_n$ surfaces did not exhibit significant calcium dependence.

Previously, photoaffinity labeling was used to determine the ligand selectivity of the interaction of $InsP_n$ with the C2B domain of Syt II (*11*). Our results were consistent with equilibrium binding assays and physiological experiments (*26*); taken together, the data suggest that $InsP_6$ is the highest-affinity ligand for the C2B domain and that the highly phosphorylated $InsP_n$s could be the most biologically relevant ligands. However, in vitro kinetic data have been unavailable for the C2B−$InsP_n$ interactions, and a controlled comparison of $InsP_n$s and $PtdInsP_n$s as ligands has not been reported.

To measure the kinetics and equilibrium dissociation constants for the C2B interaction with $InsP_n$s and $PtdInsP_n$s, we used surface plasmon resonance biosensors (*45*) with surface-linked $InsP_n$ derivatives. We found that His_6-C2B exhibited strong binding to each of the three $InsP_n$ surfaces in the following order: $Ins(1,3,4,5)P_4$ surface ($K_D = 6$ nM) > $InsP_6$ surface ($K_D = 8.5$ nM) > $Ins(1,4,5)P_3$ surface ($K_D = 14$ nM). Binding assays with radiolabeled $Ins(1,3,4,5)P_4$ showed that full-length native Syt II isolated from mouse cerebellum bound to $Ins(1,3,4,5)P_4$ with a K_D of 40 nM (*10*, *46*). The C2B domains of neuronal and non-neuronal

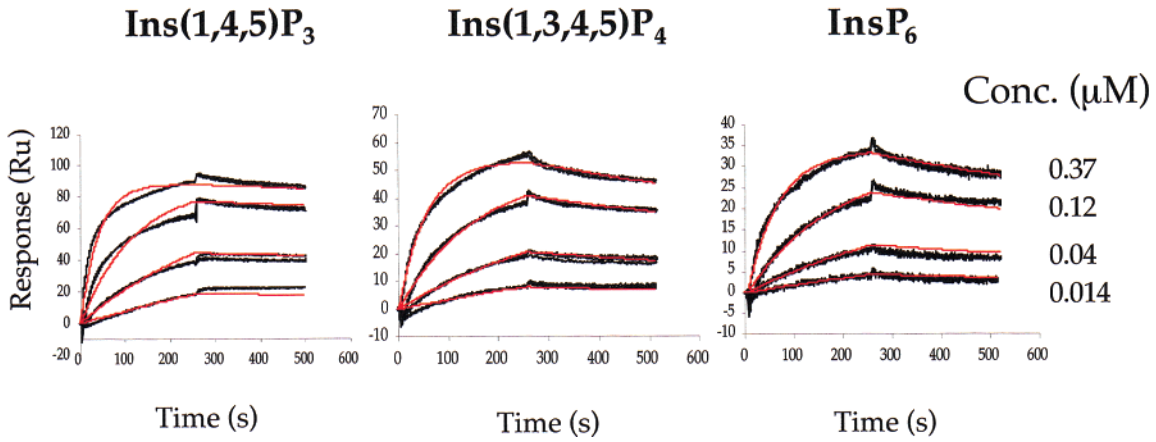

FIGURE 4: Binding of His$_6$-C2B to different InsP$_n$ surfaces at varying concentrations. The extent of binding is plotted on a sensorgram with the *y*-axis corresponding to the response (RU), while the *x*-axis corresponds to time. The protein was passed over the surface beginning at time zero and was stopped at 250 s. The flow rate was 33 μL/min.

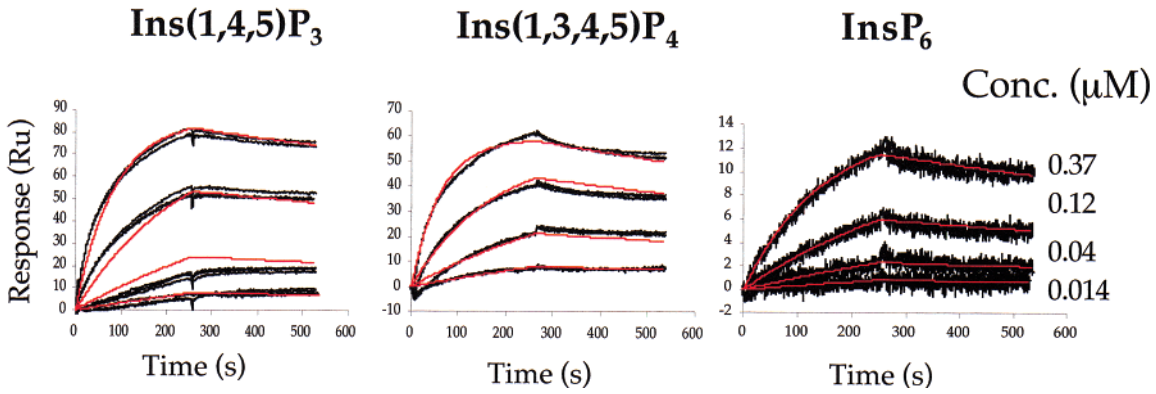

FIGURE 5: Binding of His$_6$-(C2A+C2B) to different InsP$_n$ surfaces at varying concentrations. The extent of binding is plotted on a sensorgram with the *y*-axis corresponding to the response (RU), while the *x*-axis corresponds to time (seconds). The protein was passed over the surface beginning at time zero and was stopped at 250 s. The flow rate was 33 μL/min.

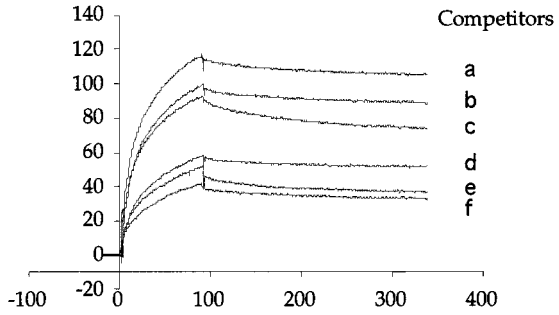

FIGURE 6: Binding of His$_6$-(C2A+C2B) to an Ins(1,3,4,5)P$_4$ surface in the presence of different competitors. His$_6$-(C2A+C2B) was incubated with different competitors (10 μM) for 15 min at 4 °C and then passed over the Ins(1,3,4,5)P$_4$ surface: (a) no competitor, (b) Ins(1,4,5)P$_3$, (c) Ins(1,3,4,5)P$_4$, (d) InsP$_6$, (e) di-C$_8$ PtdIns(4,5)-P$_2$, and (f) di-C$_8$ PtdIns(3,4,5)P$_3$.

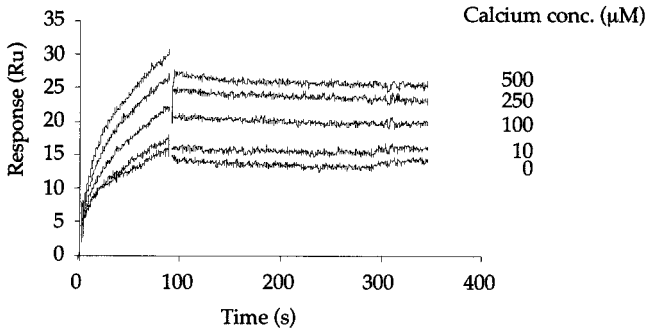

FIGURE 7: His$_6$-C2B binding to an Ins(1,3,4,5)P$_4$ surface in the presence of varying Ca^{2+} concentrations. His$_6$-C2B was incubated with varying Ca^{2+} concentrations in the presence of 1 mM Mg^{2+}, which was present in the sample as well as in the buffer. After incubation for 15 min at 4 °C, the samples were passed over the Ins(1,3,4,5)P$_4$ surface.

synaptotagmin isoforms exhibited considerable variability in their Ins(1,3,4,5)P$_4$ affinities, and much of the variation can be mapped to amino acid differences in the C-termini of these isoforms (*47*). This difference could be attributed to the use of the recombinant C2B protein instead of the native full-length Syt II protein. It is equally probable that some of the difference is due to the effect of the *P*-1-aminoalkyl tether on the sensor chip surface.

The association rates are relatively slow [$k_a = 8.1 \times 10^4$ M^{-1} s^{-1} for the Ins(1,3,4,5)P$_4$ surface] and indicate that the interactions are not simply diffusion-controlled. Perhaps conformational adjustments are required to optimize the charge−charge interactions between the tethered ligand and the mobile phase binding domain. A slow dissociation rate [$k_D = 4.9 \times 10^{-4}$ s^{-1} for Ins(1,3,4,5)P$_4$ surface] was also observed for the ligand−protein complex. In contrast, a recent study using surface plasmon resonance to study the binding of a soluble Ins(1,4,5)P$_3$ receptor binding domain and surface-immobilized Ins(1,4,5)P$_3$ reported a fast association rate ($k_a = 1.2 \times 10^6$ M^{-1} s^{-1}) and a fast dissociation rate ($k_D = 1$ s^{-1}) (*48*). Moreover, the 2-hydroxyl-linked Ins-

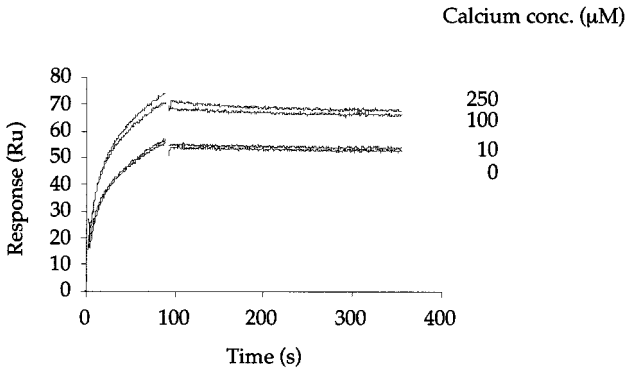

FIGURE 8: His_6-(C2A+C2B) binding to an Ins(1,3,4,5)P_4 surface in the presence of varying Ca^{2+} concentrations, as described in detail in the Figure 7 legend.

(1,4,5)P_3 surface employed in that study exhibited a >20-fold lower affinity for the Ins(1,4,5)P_3 receptor binding domain than for the free Ins(1,4,5)P_3 ligand. Since both fast and slow kinetics can be observed with different proteins on similar surfaces, these contrasting data sets demonstrate the robust nature of surface plasmon resonance for studying inositide−ligand binding.

Native Syt II contains two C2 domains, and both are required for the release of neurotransmitters from synaptic vesicles in giant squid axons (*7*, *49*). To test for the potential interaction of these two domains, a construct containing both C2 domains was expressed and evaluated. Kinetic studies on His_6-(C2A+C2B) binding to the different surfaces suggested that it also had the highest affinity for the Ins(1,3,4,5)-P_4 surface, followed by the next highest affinity for the Ins(1,4,5)P_3 surface. Interestingly, the association rate for His_6-(C2A+C2B) binding to the InsP_6 surface ($k_a = 4.6 \times 10^3$ M^{-1} s^{-1}) was 10-fold lower than that observed for the Ins(1,4,5)P_3 surface ($k_a = 3.3 \times 10^4$ M^{-1} s^{-1}) and the Ins-(1,3,4,5)P_4 surface ($k_a = 6.8 \times 10^4$ M^{-1} s^{-1}). This suggested that the extra charges due to the six phosphate groups on the inositol ring might adversely affect binding, leading to a lower association rate. It further suggested that InsP_6 might not be the actual ligand for Syt II in vivo. Since the *P*-1-(*O*-ω-alkylamino)-tethered Ins(1,4,5)P_3 and Ins(1,3,4,5)P_4 surfaces mimic PtdIns(4,5)P_2 and PtdIns(3,4,5)P_3, respectively, and have higher association rates than InsP_6, it is reasonable to propose that the PtdInsP_ns might be the preferred ligands for this protein in vivo.

We next explored the relative affinity of the C2B domain for InsP_ns and PtdInsP_ns. Protein samples were preincubated with soluble and lipid inositides and then passed over the Ins(1,3,4,5)P_4 sensor chip surface. The data showed that di-C_8 PtdIns(3,4,5)P_3 and di-C_8 PtdIns(4,5)P_2 were the most effective competitors for displacement of the binding of either the His_6-C2B or His_6-(C2A+C2B) domain to the Ins-(1,3,4,5)P_4 sensor chip. Interestingly, much less efficient displacement was observed with the soluble headgroups Ins-(1,4,5)P_3 and Ins(1,3,4,5)P_4. This suggested that in addition to having Ins(1,4,5)P_3 and Ins(1,3,4,5)P_4 displayed on the surface, the *P*-1-(*O*-ω-alkylamino) tether might also be important in contributing to recognition and binding affinity. This is consistent with the notion that the diacylglycerol moieties of PtdIns(4,5)P_2 and PtdIns(3,4,5)P_3 are important contributors to the overall binding to the His_6-C2B and His_6-(C2A+C2B) domains of Syt II.

Although the binding of InsP_ns to synaptotagmin is well-documented (*10*, *11*, *49*), how this interaction causes exocytosis is not understood (*26*). Binding of Ins(1,3,4,5)P_4 to the C2B domain inhibited both the ATP-independent Ca^{2+}-evoked release and the spontaneous release in a dose-dependent manner when injected into squid giant axon synapses (*50*). The inhibition by Ins(1,3,4,5)P_4 was completely reversed by anti-C2B antibody, suggesting that Ins-(1,3,4,5)P_4 binds to the C2B domain of synaptotagmin in vivo (*51*). These results suggest that the binding of Ins-(1,3,4,5)P_4 to the C2B domain may arrest membrane fusion by preventing the interaction of synaptotagmin with PtdInsP_ns in the plasma membrane. Interestingly, the same study also showed that the inhibitory action of Ins(1,3,4,5)P_4 binding to the C2B domain was reversed by Ca^{2+} concentrations of >50 μM (*51*). Two hypotheses can be proposed. (i) Calcium induced the binding of the C2B domain to other proteins, thereby inhibiting its interaction with PtdInsP_ns. (ii) The Ins-(1,3,4,5)P_4 binding to the C2B domain was inhibited by calcium. In the first case, an increased calcium level induced binding of the C2A domain to phospholipids (*52*) and to a plasma membrane protein, syntaxin. This binding could inhibit the C2B interaction with PtdIns(4,5)P_2 or PtdIns-(3,4,5)P_3, and thus promote the dimerization of the C2B domain or its interaction with other membrane proteins. In the second case, calcium could inhibit the binding of InsP_n to the C2B domain, thereby releasing the C2B domain to interact with other proteins.

To test these two hypotheses, the interaction of the Syt II C2B and (C2A+C2B) domains to the Ins(1,3,4,5)P_4 sensor chip was examined at varying calcium concentrations. The level of binding increased only slightly as the Ca^{2+} concentration increased. Similar effects were observed with the Ins-(1,4,5)P_3 and InsP_6-modified sensor chips. Interestingly, this result did not corroborate the calcium-dependent switch model (*12*), in which PtdIns(3,4,5)P_3-containing liposomes bound to the C2B domain of Syt I at Ca^{2+} concentrations of <10 μM, while the PtdIns(4,5)P_2-containing liposomes bound to the C2B domain at Ca^{2+} concentrations of >100 μM. The difference in results could reflect either the differing assay methodologies or molecular differences between Syt I and Syt II. Although the two isoforms exhibit a high degree of homology (75%), Syt I and Syt II could have different binding properties and different calcium sensitivities. Nonetheless, the experiments reported herein clearly suggest that the InsP_n binding level is increased in the presence of Ca^{2+}. We cannot rule out a role for C2B domain dimerization in this observed effect.

These data led to the formulation of the model illustrated in Figure 9 in which the release of neurotransmitters would occur in three stages. In the first stage (upper panel), synaptic vesicles dock onto the plasma membranes close to the active zone. The Syt II C2B domain exhibited high binding affinities for the InsP_n surfaces, a preference for PtdInsP_ns over InsP_ns, and a slow dissociation rate that was unaffected by calcium. This suggests that a Syt II C2B−PtdInsP_n interaction might be important for the docking of synaptic vesicles to the plasma membranes. The importance of this interaction is also supported by results for synaptotagmin mutants in *Drosophila melanogaster*. Both a null mutant (no synaptotagmin produced) and a point mutant in the C2B domain showed a decrease in the number of synaptic vesicles

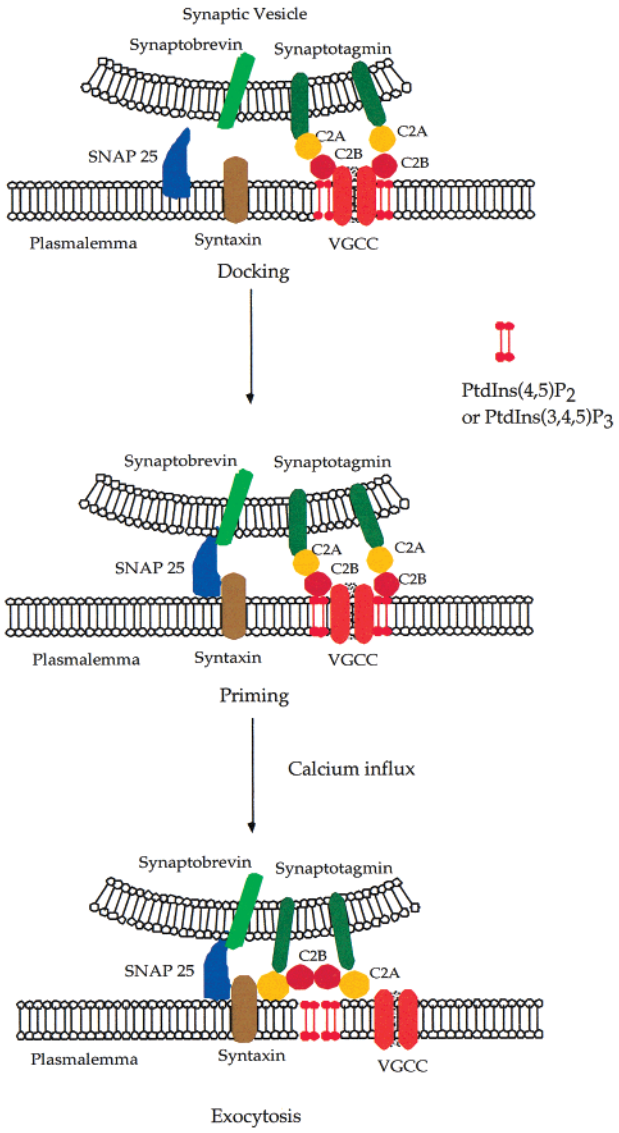

FIGURE 9: Proposed model for molecular function of Syt II during exocytosis. See the text for explanation.

morphologically docked onto the active zone (*53*), a decrease in the level of evoked neurotransmitter release, and a corresponding increase in the number of larger, undocked vesicles near synapses. The binding of the C2B domain to N-type voltage-gated calcium channels could play a role in docking the vesicles at the active zone, while the binding of the C2B domain to PtdInsP$_n$s could mediate the actual docking of the synaptic vesicles.

In the second, or priming, stage (Figure 9, middle panel), the core complex is assembled from three abundant synaptic proteins, two from the plasma membrane (syntaxin and SNAP-25) and one from synaptic vesicles (synaptobrevin). This core complex forms the anchor for a cascade of protein−protein interactions that are required for exocytosis to occur (*54*).

In the final stage (Figure 9, lower panel), calcium is released from the voltage-gated calcium channels, leading to exocytosis and a rapid release of neurotransmitters. In the presence of Ca^{2+}, the C2A domain of synaptotagmin binds to phospholipids and to syntaxin, thereby promoting C2B dimerization as well as the interaction of the C2B domain of synaptotagmin with other proteins. Recently, the binding of Syt I to negatively charged phospholipid-containing liposomes was found to be based on charge density rather than headgroup density (*52*). The anionic lipid headgroups cooperated with basic side chains surrounding Ca^{2+} in the binding site to increase the affinity for Ca^{2+}. These interactions with C2A could render the C2B domain inaccessible for binding to PtdInsP$_n$. Injection of Ins(1,3,4,5)P$_4$ at the presynaptic terminal inhibited the binding of the C2B domain with itself or with other plasma membrane proteins, thus inhibiting exocytosis. Similarly, in the presence of high calcium concentrations, the C2B domain would already have dimerized or bound to other proteins to make the Ins(1,3,4,5)P$_4$ binding site inaccessible.

Although the C2A domain exhibits calcium-dependent binding to phospholipids, this does not affect the binding of InsP$_n$ to the C2B domain. We observed no significant changes in the affinity of His$_6$-(C2A+C2B) binding to Ins(1,3,4,5)P$_4$ chip at different calcium concentrations. High-resolution multidimensional NMR studies on the C2A domain also revealed that calcium did not induce a major change in the structure of the C2A domain (*55*, *56*). Very recently, the three-dimensional structure of the (C2A+C2B) domain of Syt III was determined by X-ray crystallography (*57*), following the earlier description of the structure of the C2A domain of Syt I (*58*). The structure of the (C2A+C2B) domain did not show evidence for any communication between the C2A and the C2B domain of Syt III, consistent with our observations for the Syt II (C2A+C2B) interactions with InsP$_n$-modified biosensors as described herein. The calcium-dependent binding of the C2A domain to phospholipids apparently does not affect the binding of the C2B domain to PtdInsP$_n$, but could nonetheless affect the accessibility of the C2B domain to these PtdInsP$_n$s on the plasma membrane. Thus, it remains possible that the calcium-dependent binding of the C2A domain to phospholipids could change the orientation of the C2B domain, thus leading to the dimerization of this protein via its C2B domain or to the interaction of the C2B domain with other plasma membrane proteins.

In conclusion, biomolecular interaction analysis established the kinetics of the interactions of the C2B domains of Syt II with sensors with surface-linked InsP$_n$ ligands. The data demonstrate slow association and dissociation rates relative to those determined for the binding of the Ins(1,4,5)P$_3$ receptor with its cognate ligand. The data also show that the lipid PtdInsP$_n$s are the preferred ligands for the C2B domain, and lead to a modified model for exocytosis of synaptic vesicles in which interactions with plasma membrane phosphoinositides are important in docking, priming, and calcium-dependent neurotransmitter release.

ACKNOWLEDGMENT

We thank K. Mikoshiba and M. Fukuda (The University of Tokyo) for providing the C2B-containing plasmids, A. Chaudhary, J. Chen, and S. Ozaki for synthesis of InsP$_n$ and PtdInsP$_n$ ligands, Echelon Research Laboratories, Inc., for gifts of selected ligands, and E. M. Jorgensen for critical reading of the manuscript.

REFERENCES

1. Ullrich, B., Li, C., Zhang, J. Z., McMahon, H., Anderson, R. G. W., Geppert, M., and Südhof, T. C. (1994) *Neuron 13*, 1281−1291.

2. Schiavo, G., Osborne, S. L., and Sgouros, J. G. (1998) *Biochem. Biophys. Res. Commun. 248*, 1−8.
3. Südhof, T. C., and Rizo, J. (1996) *Neuron 17*, 379−388.
4. Perin, M. S., Fried, V. A., Mignery, G. A., Jahn, R., and Südhof, T. C. (1990) *Nature 345*, 260−261.
5. Geppert, M., Goda, Y., Hammer, R. E., Li, C., Rosahl, T. W., Stevens, C. F., and Südhof, T. C. (1994) *Cell 79*, 717−727.
6. Li, C., Ullrich, B., Zhang, J. Z., Anderson, R. G. W., Brose, N., and Südhof, T. C. (1995) *Nature 375*, 594−599.
7. Mikoshiba, K., Fukuda, M., Moreira, J. E., Lewis, F. M. T., Sugimori, M., Niinobe, M., and Llinas, R. (1995) *Proc. Natl. Acad. Sci. U.S.A. 92*, 10703−10707.
8. Shao, X., Li, C., Fernandez, I., Zhang, X., Südhof, T. C., and Rizo, J. (1997) *Neuron 18*, 133−142.
9. Chapman, E. R., Hanson, P. I., An, S., and Jahn, R. (1995) *J. Biol. Chem. 270*, 23667−23671.
10. Fukuda, M., Aruga, J., Niinobe, M., Aimoto, S., and Mikoshiba, K. (1994) *J. Biol. Chem. 269*, 29206−29211.
11. Mehrotra, B., Elliott, J. T., Chen, J., Olszewski, J. D., Profit, A. A., Chaudhary, A., Fukuda, M., Mikoshiba, K., and Prestwich, G. D. (1997) *J. Biol. Chem. 272*, 4237−4244.
12. Schiavo, G., Gu, Q.-M., Prestwich, G. D., Söllner, T. H., and Rothman, J. E. (1996) *Proc. Natl. Acad. Sci. U.S.A. 93*, 13327−13332.
13. Zhang, J. Z., Davletov, B. A., Südhof, T. C., and Anderson, R. G. W. (1994) *Cell 78*, 751−760.
14. Mizutani, A., Fukuda, M., Niinobe, M., and Mikoshiba, K. (1997) *Biochem. Biophys. Res. Commun. 240*, 128−131.
15. Jorgensen, E. M., Hartweig, E., Schuske, K., Nonet, M. L., Jin, Y., and Horvitz, H. R. (1995) *Nature 378*, 196−199.
16. Schiavo, G., Gmachi, M. J. S., Steinbeck, G., Söllner, T. H., and Rothman, J. E. (1995) *Nature 378*, 733−736.
17. Schiavo, G., Stenbeck, G., Rothman, J. E., and Söllner, T. H. (1997) *Proc. Natl. Acad. Sci. U.S.A. 94*, 997−1001.
18. Mehta, P. P., Battenberg, E., and Wilson, M. C. (1996) *Proc. Natl. Acad. Sci. U.S.A. 93*, 10471−10476.
19. Sheng, Z. H., Yokoyama, C. T., and Catterall, W. A. (1997) *Proc. Natl. Acad. Sci. U.S.A. 94*, 5405−5410.
20. Kim, D. K., and Catterall, W. A. (1997) *Proc. Natl. Acad. Sci. U.S.A. 94*, 14782−14786.
21. Brose, N., Petrenko, A. G., Südhof, T. C., and Jahn, R. (1992) *Science 256*, 1021−1025.
22. Chapman, E. R., An, S., Edwardson, J. M., and Jahn, R. (1996) *J. Biol. Chem. 271*, 5844−5849.
23. Osborne, S. L., Herreros, J., Bastiaens, P. I., and Schiavo, G. (1999) *J. Biol. Chem. 274*, 59−66.
24. Prestwich, G. D. (1996) *Acc. Chem. Res. 29*, 503−513.
25. Prestwich, G. D., Dormán, G., Elliott, J. T., Marecak, D. M., and Chaudhary, A. (1997) *Photochem. Photobiol. 65*, 222−234.
26. Fukuda, M., and Mikoshiba, K. (1997) *BioEssays 19*, 593−603.
27. Chen, J., and Prestwich, G. D. (1996) *J. Labelled Compd. Radiopharm. 38*, 1113−1119.
28. Dormán, G., Chen, J., and Prestwich, G. D. (1995) *Tetrahedron Lett. 36*, 8719−8722.
29. Estevez, V. A., and Prestwich, G. D. (1991) *J. Am. Chem. Soc. 113*, 9885−9887.
30. Marecek, J. F., and Prestwich, G. D. (1991) *Tetrahedron Lett. 32*, 1863−1866.
31. Chen, J., Profit, A. A., and Prestwich, G. D. (1996) *J. Org. Chem. 61*, 6305−6312.
32. O'Shannessy, D. J., Brigham-Burke, M., and Peck, K. (1992) *Anal. Biochem. 205*, 132−136.
33. Prestwich, G. D., Chaudhary, A., Chen, J., Feng, L., Mehrotra, B., and Peng, J. (1999) in *Phosphoinositides: Chemistry, Biochemistry and Biomedical Applications* (Bruzik, K. S., Ed.) Vol. 818, pp 24−37, American Chemical Society, Washington, DC.
34. Theibert, A. B., Prestwich, G. D., Jackson, T. R., and Hammonds-Odie, L. P. (1997) in *Signaling by Inositol Lipids and Inositol Phosphates* (Shears, S. B., Ed.) pp 117−150, Oxford University Press, Oxford, U.K.
35. Mourey, R. J., Estevez, V. A., Marecek, J. F., Barrow, R. K., Prestwich, G. D., and Snyder, S. H. (1993) *Biochemistry 32*, 1719−1726.
36. Estevez, V. A., and Prestwich, G. D. (1991) *Tetrahedron Lett. 32*, 1623−1626.
37. Inoue, T., Kikuchi, K., Hirose, K., Iino, M., and Nagano, T. (1999) *Bioorg. Med. Chem. Lett. 9*, 1697−1702.
38. Hammonds-Odie, L. P., Jackson, T. R., Profit, A. A., Blader, I. J., Turck, C. W., Prestwich, G. D., and Theibert, A. B. (1996) *J. Biol. Chem. 271*, 18859−18868.
39. Theibert, A. B., Estevez, V. A., Ferris, C. D., Danoff, S. K., Barrow, R. K., Prestwich, G. D., and Snyder, S. H. (1991) *Proc. Natl. Acad. Sci. U.S.A. 88*, 3165−3169.
40. Abdullah, M., Hughes, P. J., Craxton, A., Gigg, R., Marecek, J. F., Prestwich, G. D., and Shears, S. B. (1992) *J. Biol. Chem. 267*, 22340−22345.
41. Voglmaier, S. M., Bembenek, M. E., Kaplin, A. I., Dormán, G., Olszewski, J. D., Prestwich, G. D., and Snyder, S. H. (1996) *Proc. Natl. Acad. Sci. U.S.A. 93*, 4305−4310.
42. Myszka, D. G., Morton, T. A., Doyle, M. L., and Chaiken, I. M. (1997) *Biophys. Chem. 64*, 127−137.
43. Myszka, D. G., and Morton, T. A. (1998) *Trends Biochem. Sci. 23*, 149−150.
44. Mikoshiba, K., Fukuda, M., Ibata, K., Kabayama, H., and Mizutani, A. (1999) *Chem. Phys. Lipids 98*, 59−67.
45. Morton, T., and Myszka, D. (1998) *Methods Enzymol. 295*, 268−294.
46. Niinobe, M., Yamaguchi, Y., Fukuda, M., and Mikoshiba, K. (1994) *Biochem. Biophys. Res. Commun. 205*, 1036−1042.
47. Ibata, K., Fukuda, M., and Mikoshiba, K. (1998) *J. Biol. Chem. 273*, 12267−12273.
48. Natsume, T., Hirota, J., Yoshikawa, F., Furuichi, T., and Mikoshiba, K. (1999) *Biochem. Biophys. Res. Commun. 260*, 527−533.
49. Fukuda, M., Moreira, J. E., Lewis, F. M. T., Sugimori, M., Niinobe, M., Mikoshiba, K., and Llinas, R. (1995) *Proc. Natl. Acad. Sci. U.S.A. 92*, 10708−10712.
50. Llinas, R., Sugimori, M., Lang, E. J., Morita, M., Fukuda, M., Niinobe, M., and Mikoshiba, K. (1994) *Proc. Natl. Acad. Sci. U.S.A. 91*, 12990−12993.
51. Ohara-Imaizumi, M., Fukuda, M., Niinobe, M., Misonou, H., Ikeda, K., Murakami, T., Kawasaki, M., Mikoshiba, K., and Kumakura, K. (1997) *Proc. Natl. Acad. Sci. U.S.A. 94*, 287−291.
52. Zhang, X., Rizo, J., and Südhof, T. (1998) *Biochemistry 37*, 12395−12403.
53. Reist, N. E., Buchanan, J., Li, J., DiAntonio, A., Buxton, E. M., and Schwarz, T. L. (1998) *J. Neurosci. 18*, 7662−7673.
54. Linial, M. (1997) *J. Neurochem. 69*, 1781−1792.
55. Shao, X., Fernandez, I., Südhof, T. C., and Rizo, J. (1998) *Biochemistry 37*, 16106−16115.
56. Ubach, J., Zhang, X., Shao, X., Südhof, T. C., and Rizo, J. (1998) *EMBO J. 17*, 3921−3930.
57. Sutton, R. B., Ernst, J. A., and Brunger, A. T. (1999) *J. Cell Biol. 147*, 589−598.
58. Sutton, R. B., Davletov, B. A., Berghuis, A. M., Südhof, T. C., and Sprang, S. R. (1995) *Cell 80*, 929−938.

BI000487O